Molecular Biology of the Cell
Vol. 11, 3161–3177, November 1998

Biogenesis of Polarized Epithelial Cells During Kidney Development In Situ: Roles of E-Cadherin–mediated Cell–Cell Adhesion and Membrane Cytoskeleton Organization

Peter A. Piepenhagen* and W. James Nelson†

Department of Molecular and Cellular Physiology, Stanford University School of Medicine, Stanford, California 94305-5345

Submitted July 1, 1998; Accepted August 19, 1998
Monitoring Editor: Caroline Damsky

Organization of proteins into structurally and functionally distinct plasma membrane domains is an essential characteristic of polarized epithelial cells. Based on studies with cultured kidney cells, we have hypothesized that a mechanism for restricting Na/K-ATPase to the basal-lateral membrane involves E-cadherin–mediated cell–cell adhesion and integration of Na/K-ATPase into the Triton X-100–insoluble ankyrin- and spectrin-based membrane cytoskeleton. In this study, we examined the relevance of these in vitro observations to the generation of epithelial cell polarity in vivo during mouse kidney development. Using differential detergent extraction, immunoblotting, and immunofluorescence histochemistry, we demonstrate the following. First, expression of the 220-kDa splice variant of ankyrin-3 correlates with the development of resistance to Triton X-100 extraction for Na/K-ATPase, E-cadherin, and catenins and precedes maximal accumulation of Na/K-ATPase. Second, expression of the 190-kDa slice variant of ankyrin-3 correlates with maximal accumulation of Na/K-ATPase. Third, Na/K-ATPase, ankyrin-3, and fodrin specifically colocalize at the basal-lateral plasma membrane of all epithelial cells in which they are expressed and during all stages of nephrogenesis. Fourth, the relative immunofluorescence staining intensities of Na/K-ATPase, ankyrin-3, and fodrin become more similar during development until they are essentially identical in adult kidney. Thus, renal epithelial cells in vivo regulate the accumulation of E-cadherin–mediated adherens junctions, the membrane cytoskeleton, and Na/K-ATPase through sequential protein expression and assembly on the basal-lateral membrane. These results are consistent with a mechanism in which generation and maintenance of polarized distributions of these proteins in vivo and in vitro involve cell–cell adhesion, assembly of the membrane cytoskeleton complex, and concomitant integration and retention of Na/K-ATPase in this complex.

INTRODUCTION

Development and maintenance of polarized epithelia are crucial for all multicellular animals. Epithelia participate in important morphogenetic events during development, permit the formation of different bodily compartments, and carry out vectorial transport between these different compartments. Cells comprising epithelial monolayers are able to accomplish these functions because they are adherent and functionally polarized. Na/K-ATPase plays an important and widespread role in epithelial transport processes and has been used as a model protein to study sorting processes (Rodriguez-Boulan and Nelson, 1989). Na/K-ATPase establishes and maintains transepithelial Na^+ gradients, which both control movement of water

* Present address: Department of Cell Biology, Yale University School of Medicine, New Haven, CT 06510.
† Corresponding author. E-mail address: wjnelson@leland.stanford.edu.

and provide energy for secondary active transport processes (Vander, 1995). Depending on whether epithelia are secretory (e.g., choroid plexus) or reabsorptive (e.g., kidney), Na/K-ATPase can be localized to either apical or basal-lateral plasma membranes, respectively (Kashgarian *et al.*, 1985; Marrs *et al.*, 1993). In kidney, the activity and polarized distribution of Na/K-ATPase are essential for reabsorption of ions and other small molecules from the ultrafiltrate and for concentration of urine (Katz *et al.*, 1979; Torretti *et al.*, 1972; Vander, 1995).

Previous studies using cultured Madin–Darby canine kidney (MDCK) cells as a model of polarized renal epithelia have described two intracellular sites at which sorting of Na/K-ATPase occurs. One of these is the trans-Golgi network (TGN) in which a variable amount (50–80%) of newly synthesized Na/K-ATPase is sorted into transport vesicles that are delivered directly to the basal-lateral plasma membrane (Caplan *et al.*, 1986; Mays *et al.*, 1995). The other site of sorting is the plasma membrane where Na/K-ATPase delivered to the basal-lateral plasma membrane is selectively stabilized and retained, whereas Na/K-ATPase delivered to the apical membrane is rapidly internalized and degraded (Hammerton *et al.*, 1991). In theory, sorting at either site could operate alone to generate a polarized plasma membrane distribution of Na/K-ATPase. Previous results, however, indicate that although the fidelity of plasma membrane sorting is sufficient to generate observed cell surface polarity of Na/K-ATPase, the fidelity of TGN sorting is not (Mays *et al.*, 1995). Generation and maintenance of a polarized distribution of Na/K-ATPase appear to require plasma membrane sorting, regardless of whether this occurs alone or in concert with TGN sorting. Selective stabilization of basal-lateral membrane Na/K-ATPase is thought to occur through direct interaction with the ankyrin- and spectrin-based membrane cytoskeleton. This structure is localized specifically beneath basal-lateral plasma membranes in MDCK cells (Nelson and Veshnock, 1986) and renal epithelia (Morrow *et al.*, 1989; Piepenhagen *et al.*, 1995). Purified Na/K-ATPase and ankyrin have been shown to bind in vitro (Nelson and Veshnock, 1987; Davis and Bennett, 1990a,b; Devarajan *et al.*, 1994), and a high-molecular-weight complex of Na/K-ATPase, ankyrin, and fodrin (nonerythroid spectrin) has been isolated from MDCK cells (Nelson and Hammerton, 1989).

A restricted subcellular distribution of the membrane cytoskeleton requires positional information from transmembrane protein(s). E-cadherin appears to provide this information. Transfection of full-length E-cadherin into cadherin-deficient fibroblasts causes the reorganization of the membrane cytoskeleton and Na/K-ATPase to sites of cell–cell contact (McNeill *et al.*, 1990). Furthermore, complexes containing E-cadherin, ankyrin, and fodrin have been isolated from MDCK cells (Nelson *et al.*, 1990). These results suggest that interactions between E-cadherin and the membrane cytoskeleton provide the spatial cue to organize the membrane cytoskeleton specifically beneath basal-lateral plasma membranes. Although not directly demonstrated, this interaction likely involves direct or indirect binding of the membrane cytoskeleton to the E-cadherin–associated proteins α- and β-catenin (Herrenknecht *et al.*, 1991; Nagafuchi *et al.*, 1991; Knudsen and Wheelock, 1992; Peifer *et al.*, 1992; Piepenhagen and Nelson, 1993).

A necessary test of these mechanisms identified in cultured kidney epithelial cells is to examine the spatiotemporal regulation of Na/K-ATPase expression and subcellular organization in situ during kidney development. Development of kidney nephrons begins on embryonic day 11.5 in the mouse when the ureteric bud first contacts the metanephric mesenchyme. This interaction induces small groups of nonpolarized mesenchymal cells surrounding the ureteric bud to adhere tightly to one another and begin to differentiate into polarized epithelial cells (Vestweber *et al.*, 1985). Nephrogenic structures comprising differentiating epithelial cells undergo a series of stereotyped morphological changes including comma- and S-shaped body stages, fuse with the developing ureteric system, and differentiate into the structures and segments found in mature nephrons. Interaction of ureteric buds with metanephric mesenchyme also induces ureteric buds to branch and further invade the mesenchyme. This results in structures in many different stages of differentiation being present within a single embryonic kidney (for more detailed reviews of kidney development, see Saxen and Sariola, 1987; Ekblom, 1989).

In a previous report (Piepenhagen *et al.*, 1995), we documented a correlation among subcellular distributions and relative immunofluorescence staining intensities of Na/K-ATPase, ankyrin-3, and fodrin along adult mouse kidney nephrons. We now examine protein expression, localization, and association with the cytoskeleton during kidney development using differential detergent extraction, immunoblotting, and immunofluorescence microscopy. Our results are the first quantitative study of the patterns of Na/K-ATPase, ankyrin, fodrin, and catenin expression during early stages of renal epithelial development. They provide new insight into mechanisms of protein sorting in situ, support a generalized mechanism for generating cell polarity, and have implications for understanding pathological states in which epithelial protein sorting appears to be perturbed.

MATERIALS AND METHODS

Antibodies

The Troma-1 rat monoclonal supernatant used to detect cytokeratin 8 was obtained from the National Institutes of Health Developmental Studies Hybridoma Bank (Department of Biology, University of Iowa, Iowa City, IA; under contract N01-HD-2-3144 from the National Institute of Child Health and Human Development) and has been characterized previously (Brulet *et al.*, 1980; Kemler *et al.*, 1981); the supernatant was used at a dilution of 1:2 to stain kidney sections. The rabbit polyclonal antiserum used to detect Na/K-ATPase recognizes the large H5 cytoplasmic loop of sheep Na/K-ATPase α-subunit. It was raised in this laboratory and has been described previously (Piepenhagen *et al.*, 1995); it was used at a dilution of 1:500 for immunofluorescence and at a dilution of 1:1000 for immunoblotting. The C4CB/6B mouse monoclonal supernatant used to detect Na/K-ATPase is specific for the α-subunit and was a gift from Drs. Kent Grindstaff and Robert Mercer (Washington University, St. Louis, MO); supernatant was used a dilution of 1:5 for immunofluorescence. The rabbit polyclonal antiserum directed against the α-subunit of fodrin (nonerythroid spectrin) was raised in this laboratory and has been described in prior studies (Nelson and Veshnock, 1986); it was used at a dilution of 1:150 for immunofluorescence and at a dilution of 1:1000 for immunoblotting. The rabbit polyclonal antiserum used to detect ankyrin-3 was a gift from Drs. Luanne Peters and Sam Lux (Harvard Medical School, Boston, MA) and has been described previously (Peters *et al.*, 1995; Piepenhagen *et al.*, 1995); it was used at a dilution of 1:500 for immunofluorescence and at a dilution of 1:1000 for immunoblotting. The antiserum specific for the extracellular domain of E-cadherin was a gift from Dr. Rolf Kemler (Max-Planck Institut für Immunobiologie, Freiburg Germany) and has been characterized previously (Vestweber and Kemler, 1984; Vestweber *et al.*, 1985); it was used at a dilution of 1:500 for both immunofluorescence and immunoblotting. The rabbit polyclonal antiserum directed against the cytoplasmic domain of E-cadherin was raised in this laboratory to a fusion protein of glutathione *S*-transferase and the complete cytoplasmic domain of mouse E-cadherin; this antibody shows general reactivity toward type I cadherins (Marrs *et al.*, 1993). E-cadherin cytoplasmic domain fusion protein was isolated from bacteria and purified by binding it to glutathione-agarose, washing extensively, subjecting bound protein to preparative SDS-PAGE, and then electroeluting the appropriately sized protein band. Electroeluted protein was used to inject rabbits and generate serum that was then ammonium sulfate cut; it was used at a dilution of 1:1000 for immunoblotting. Rabbit polyclonal antiserum directed against a α-catenin peptide sequence was raised in this laboratory and has been described previously (Nathke *et al.*, 1994); it was used at a dilution of 1:500 for immunofluorescence and immunoblotting. The rabbit polyclonal antiserum directed against β-catenin was raised in this laboratory and has been described previously (Hinck *et al.*, 1994); it was used at a dilution of 1:500 for both immunofluorescence and immunoblotting. The rabbit polyclonal antiserum directed against plakoglobin was raised in this laboratory and has been described in prior studies (Nathke *et al.*, 1994); it was used at a dilution of 1:500 for both immunofluorescence and immunoblotting. Desmoplakin expression was examined using a rabbit polyclonal antiserum raised in this laboratory against desmoplakin purified from bovine snouts (Pasdar and Nelson, 1988); it was used at a dilution of 1:500 for immunofluorescence. ZO-1 expression was examined using a mixture of rat monoclonal antibodies R26.4C and R40.76 that specifically react with this protein, as previously described (Anderson *et al.*, 1988; Stevenson *et al.*, 1986). R26.4C hybridoma supernatant was purchased from the National Institutes of Health Developmental Studies Hybridoma Bank, and R40.76 ascites generated from the corresponding hybridoma line was purchased from Chemicon (Temecula, CA); R26.4C supernatant was used at a dilution of 1:2 for immunofluorescence, and R40.76 ascites was used at a dilution of 1:500 for immunofluorescence.

Animal Breeding and Microdissection of Kidneys from Embryonic and Postnatal Mice

Male and female mice (8–10 wk old) of strain CD1 and C57BL/6 were purchased from Charles River Laboratories (Wilmington, MA). Male and female mice in a ratio of 1:2 were placed in cages together at ~7:00 PM. Twelve hours later, females were examined for vaginal plugs. Females with vaginal plugs were removed to separate marked cages (3–4 mice per cage); if positive identification of vaginal plugs was difficult, females were assumed to have mated and were removed. Females possessing vaginal plugs were assumed to have mated at 1:00 AM, and the morning on which vaginal plugs were detected was designated day 0. For embryonic time points, pregnant females were killed after the appropriate numbers of days by cervical dislocation. Embryos within their amniotic sacs were removed from killed females and placed into a Petri dish filled with ice-cold DMEM supplemented with 10% FCS. Embryos were removed from amniotic sacs and pinned in the anatomical position on top of a glass Petri dish filled with paraffin wax. A Zeiss (Thornwood, NY) stemi SR stereoscopic dissecting microscope and fiber optic light source were then used to view pinned embryos. For early postnatal time points, pups were killed by decapitation and were pinned as above. Microdissecting forceps were used to open the abdominal cavity and remove the kidneys, which were placed into a 35-mm Petri dish filled with DMEM supplemented with 10% FCS. In the case of 4- and 8-wk-old postnatal mice, animals were killed by cervical dislocation. Kidneys were removed using dissecting forceps without the aid of a dissecting microscope and were placed into a 100-mm Petri dish filled with DMEM supplemented with 10% FCS. Once all kidneys from a litter of embryonic mice or an appropriate number of postnatal mice had been obtained, extraneous fat, connective tissue, and most of the ureter were removed. Kidneys were then washed by sequentially transferring them to two separate Petri dishes filled with ice-cold PBS (2.7 mM KCl, 1.5 mM KH_2PO_4, 137 mM NaCl, and 8 mM NaH_2PO_4) by gently swirling in the Petri dishes for ~30 s. After kidneys had been washed, they were immediately homogenized and processed for immunofluorescence, or frozen. Freezing was accomplished by placing kidneys into a drop of PBS on a piece of aluminum foil and then placing the piece of aluminum foil on top of an aluminum block that had been equilibrated with a bed of dry ice on which it was sitting. Frozen kidneys were stored at −80°C until enough tissue had been obtained to generate total protein homogenates for embryonic time points.

Preparation of Total Protein Homogenates

Kidneys from mice of various ages were placed into ice-cold SDS extraction buffer (1% SDS, 10 mM Tris-HCl, pH 7.5, 2 mM EDTA, 1 mM pefabloc [Boehringer Mannheim, Indianapolis, IN], 1 mM dithiothreitol [DTT], 0.7 μg/ml pepstatin, 0.1 mM leupeptin, and 1 mM *N*α-*p*-tosyl-L-lysine chloromethyl ketone); 1 ml extraction buffer was used for each time point. Approximate numbers of kidneys used for each developmental age were as follows: embryonic day 12 (E12) (170), E13 (150), E14 (100), E15 (70), E16 (50), E17 (40), E18 (30), E19 (25), neonatal (16) 1 wk (6), 2 wk (4), 4 wk (2), and 8 wk (0.5). Kidneys from postnatal time points were placed into homogenization buffer immediately after dissection and washing, whereas frozen kidneys from embryonic time points were first thawed in ice-cold PBS. Kidneys from 4- and 8-wk-old mice were cut into smaller pieces (3–4 mm^2) before being placed into extraction buffer, whereas kidneys from earlier developmental ages were left intact. Tissue pieces in extraction buffer were then homogenized by sonication at 4°C (constant duty cycle, 30% power, three 10-s bursts using a Branson Ultrasonics (Danbury, CT) 250 Sonifier equipped with a microtip). Tissue homogenate was aliquoted, flash frozen in liquid N_2, and stored at −80°C.

Preparation of Triton X-100–soluble and –insoluble Fractions

Kidneys from mice of various ages were placed into CSK extraction buffer (50 mM NaCl, 300 mM sucrose, 10 mM piperazine-*N*,*N*′-bis[2-ethanesulfonic acid], pH 6.8, 3 mM MgCl, 0.5% Triton X-100, 1 mM pefabloc, 1 mM DTT, 0.7 μg/ml pepstatin, 0.1 mM leupeptin, and 1 mM *Nα-p*-tosyl-L-lysine chloromethyl ketone); 1 ml extraction buffer was used for each time point. Approximate numbers of kidneys used for each developmental age were as follows: E16 (25), E17 (20), E18 (16), E19 (22), neonatal (18), 1 wk (6), 2 wk (4), 4 wk (2), and 8 wk (0.5). In all cases, kidneys were placed into homogenization buffer immediately after dissection and washing. Kidneys from 4- and 8-wk-old mice were cut into smaller pieces (3–4 mm^2) before being placed into extraction buffer, whereas kidneys from earlier developmental ages were left intact. Tissue pieces in extraction buffer were then homogenized by sonication at 4°C as described above. Tissue homogenate was centrifuged at 15,000 × *g* for 15 min to generate a supernatant and pellet. After centrifugation, the supernatant was removed with a pipette and transferred to a different tube on ice. The pellet was then resuspended by adding 1 ml SDS extraction buffer and sonicating at 4°C. Volumes of the supernatant and pellet fractions were measured with a pipetteman, and more CSK or SDS extraction buffer was added, if necessary, to adjust the two fractions to the same final volume. Triton X-100–soluble and –insoluble fractions were then aliquoted, flash frozen in liquid N_2, and stored at −80°C.

Immunoblotting

Aliquots of total protein homogenate or Triton X-100–soluble and –insoluble fractions were thawed on ice and mixed with 4× SDS sample buffer to yield samples consisting of tissue homogenate in 1× SDS sample buffer (2% SDS, 40 mM Tris-HCl, pH 6.8, 7.5% glycerol, 50 mM DTT, and 0.1% bromphenol blue). Samples were denatured at 65°C for 15 min and subjected to SDS-PAGE using polyacrylamide gels of various concentrations. For total protein homogenates, 40 μg of total protein (measured using the BCA assay, Pierce Chemical, Rockford, IL) were loaded per lane. For Triton X-100–soluble and –insoluble fractions, equal volumes (5–20 μl) were loaded for each developmental age. In all cases, a single sample was prepared for each developmental age and/or fraction and split equally among different gels; each set of analyses was performed at least three times with identical results. Gels were electroblotted to nitrocellulose filters at 4°C for 4 h at 250 mA constant current (transfer buffer consisted of 20 mM Tris-acetate, pH 8.3, 0.1% SDS, and 20% isopropanol). After transfer, nitrocellulose filters were fixed in 50% isopropanol for 20 min, washed twice in deionized H_2O for 10 min, and then stained with Ponceau S to detect molecular weight standards. Nitrocellulose filters were blocked overnight at room temperature in a solution consisting of 1% normal goat serum, 3% BSA, and 5% nonfat dry milk in gelatin wash buffer (150 mM Tris-HCl, pH 7.5, 1.3 M NaCl, 50 mM NaN_3, 10 mM EDTA, 1% Tween 20, and 0.1% gelatin). Nitrocellulose filters were then incubated with antisera diluted in blocking buffer without normal goat serum overnight at 4°C. Nitrocellulose filters were next washed four times in gelatin wash buffer for 15 min each at room temperature and then incubated with 0.1 μCi/lane ^{125}I-labeled goat anti-rabbit secondary antibody diluted in gelatin wash buffer for 2 h at room temperature. Finally, nitrocellulose filters were washed six times in gelatin wash buffer for 15 min each at room temperature, allowed to air dry, and subjected to autoradiography. Band intensity on autoradiograms was quantified using a GS 300 scanning densitometer (Hoefer Science Instruments, San Francisco, CA) and Microsoft Excel (Microsoft, Redmond, WA). For preparation of Figures 1 and 2, autoradiograms were digitized and imported into Adobe Photoshop (Adobe Systems, Mountain View, CA) using a Hewlett Packard Scanjet IIc scanner (Hewlett-Packard, Greeley, CO). Autoradiograms were cropped, arranged, and labeled using Adobe Photoshop (Mountain View, CA) and then printed directly from the computer file using a Tektronix Phaser 440 photo-digital printer (Ada, Irvine, CA); the reproduced blots are an accurate representation of the original autoradiograms.

Tissue Preparation for Immunofluorescence

Kidneys from mice of various developmental ages were fixed in 10 ml paraformaldehyde-lysine-periodate fixative (McClean and Nakane, 1974) on ice for 30 min immediately after dissection and washing. Kidneys from 4- and 8-wk-old mice were cut into halves and quarters, respectively, before fixation, whereas kidneys from earlier developmental ages were left intact. After fixation, tissue was washed three times with ice-cold PBS for 10 min at 4°C. After this step, tissue was cryoprotected by transferring it to a conical tube containing 2.5 M sucrose in PBS. For 4- and 8-wk-old kidneys, a 50-ml tube containing 40 ml sucrose solution was used, whereas a 14-ml tube filled with 10 ml sucrose solution was used for all earlier developmental ages. Tissue was allowed to remain in this solution for 48 h at 4°C, after which it was transferred to a fresh tube of 2.5 M sucrose in PBS for long-term storage at 4°C. Tissue was stable in this condition for several months. As required, tissue was removed from the 2.5 M sucrose solution, immersed in OCT cryo-embedding compound (Miles Diagnostics, Kankakee, IL), and flash frozen in liquid N_2. Frozen tissue blocks were then mounted onto chucks and trimmed while on a bed of dry ice. Trimmed blocks were sectioned using a 2800 Frigocut N cryostat (Reichert-Jung, Cambridge Instruments GmbH, Nussloch, Germany), and 5 μm-thick sections were transferred onto Superfrost Plus glass microscope slides (Fisher Scientific, Pittsburgh, PA).

Immunofluorescence Staining

Frozen sections (5 μm thick) were allowed to warm to room temperature and were then extracted for 15 s with CSK buffer. The slides were then washed twice with PBS at room temperature; each wash was carried out for 5 min. After this step, slides were incubated in blocking solution for 2 h at room temperature in humidified chambers. For slides being stained with rabbit antisera, the blocking solution consisted of PBS containing 20% normal goat serum, 0.2% BSA, 50 mM NH_4Cl, 25 mM glycine, and 25 mM lysine. For slides being stained with rat monoclonal antibodies, this blocking solution was supplemented with a 1:10 dilution of goat anti-rat unlabeled secondary antibody; for slides being stained with mouse monoclonal antibodies, the blocking solution was supplemented with a 1:5 dilution of unlabeled goat anti-mouse secondary antibody. Inclusion of unlabeled anti-rat and anti-mouse secondary antibodies in the blocking solution was required to prevent nonspecific binding of the labeled anti-rat and anti-mouse secondary antibodies to basement membranes in kidney. Blocking of this nonspecific binding was demonstrated to be effective by omitting primary antibody and staining sections with mouse and rat secondary antibodies alone; such slides showed only faint autofluorescence, which was observed when secondary antibodies were omitted. After the slides were blocked, they were washed twice with PBS containing 0.2% BSA. The washes were carried out for 10 min at room temperature. The slides were then incubated with the appropriate primary antibody solutions overnight at 4°C in humidified chambers. Primary antibodies were diluted in PBS containing 20% normal goat serum and 0.2% BSA; for double-labeling experiments, both primary antibodies were incubated with sections at the same time. The following day, slides were again washed twice with PBS containing 0.2% BSA. Both washes were conducted for 10 min at room temperature. The slides were then incubated with the appropriate secondary antibody solutions for 2 h at room temperature in humidified chambers; for double-labeling experiments, both secondary antibodies were incubated with sections at the same time. All rhodamine- and fluorescein-conjugated secondary antibodies were diluted 1:200 in PBS containing 20% normal goat serum and 0.2% BSA.

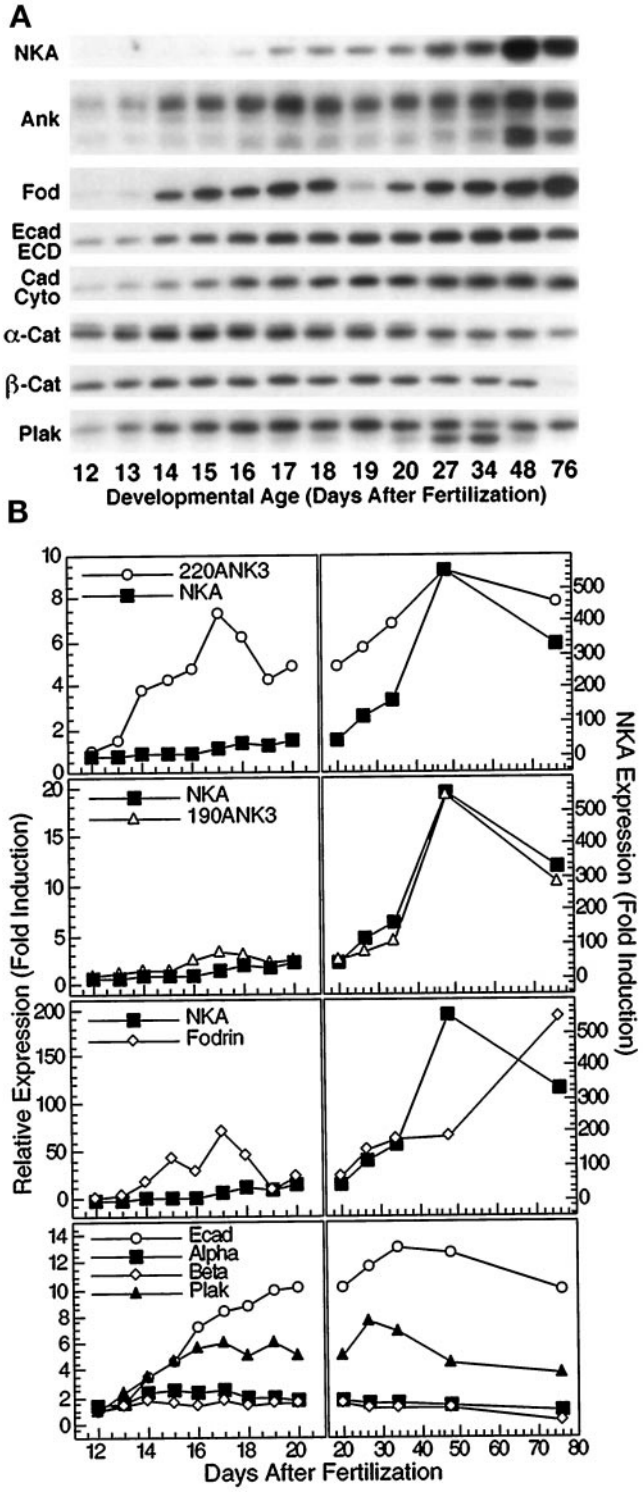

Figure 1. Protein expression patterns during kidney development. (A) Whole mouse kidney homogenates (40 μg total protein/lane) from CD1 mice of various embryonic and postnatal ages were separated on 5% (ank3 and fod) or 7.5% (NKA, Ecad ECD, Ecad Cyto, α-cat, β-cat, and plak) SDS-polyacrylamide gels and then electroblotted to nitrocellulose filters. Nitrocllue filters were probed with polyclonal antibodies specific for Na/K-ATPase (NKA), ankyrin-3 (Ank3), nonerythroid spectrin (fodrin, fod), E-cadherin extracellular domain (Ecad ECD), E-cadherin cytoplasmic domain (Ecad Cyto), α-catenin (α-cat), β-catenin (β-cat), or plakoglobin (plak). Specific protein bands at appropriate molecular sizes were observed in all cases. Ankyrin-3 immunoblot shows both 190-kDa (lower doublet) and 220-kDa (upper band) splice variants of Ankyrin-3. (B) Autoradiograms shown in A were subjected to scanning densitometry. Resulting band intensities are expressed as fold induction relative to weakest signal obtained (usually at E12) and plotted against developmental age (days after fertilization). Left, time points before birth; right, time points after birth. For the sake of comparison, data for Na/K-ATPase are replotted together with those for the 220- and 190-kDa splice variants of ankyrin-3 and fodrin. Data for E-cadherin, α-catenin, β-catenin, and plakoglobin are plotted in the bottom two panels. Antisera directed against extracellular and cytoplasmic domains of E-cadherin detected single bands of identical molecular sizes (~120 kDa), which displayed similar expression profiles. Therefore, expression data for the two were averaged, and the resulting averaged data are shown in the bottom two panels (Ecad).

After the secondary antibody incubation, slides were washed twice in PBS containing 0.2% BSA as above and then mounted with glass coverslips in PBS containing 16.7% Mowoil (Calbiochem, San Diego, CA), 33% glycerol, and 0.1% paraphenylene diamine. Slides were viewed and photographed using a Zeiss Axioplan epifluorescence microscope. For preparation of Figures 3 and 4, photographic slides (Kodak Ektachrome ASA 400, Eastman Kodak, Rochester, NY) were scanned onto a Kodak photo-digital compact disk (α CD Imaging, Palo Alto, CA). Photographic images were then imported from photo compact discs into Adobe Photoshop and arranged and labeled. Final Figures 3 and 4 were then printed directly from computer files using a photo-digital printer as described above; the reproduced images are accurate representations of the original images.

RESULTS

Patterns of Protein Expression During Kidney Development

Protein levels of Na/K-ATPase, ankyrin-3, fodrin, E-cadherin, α-catenin, β-catenin, and plakoglobin were examined during mouse kidney development by Western blotting. Data from the analysis of CD1 mice are shown (Figure 1); protein expression was also examined in C57Bl/6 mice, and similar trends in protein expression were observed. Expression of ankyrin-3 was specifically examined because it has been shown to be the major ankyrin isoform expressed in renal epithelia (Peters *et al.*, 1995). In kidney, processing of ankyrin-3 pre-mRNA results in five major splice variant proteins that can be easily identified by their size (110, 114, 150, 190, and 220 kDa). Expression patterns of the three smallest splice variants (110, 114, and 150 kDa) are not shown. Their expression profiles were completely dissimilar from those of Na/K-ATPase, fodrin, and the 190- and 220-kDa splice variants of ankyrin-3. In addition, recent data have indicated that the 110- and 114-kDa splice variants are associated with lysosomes rather than plasma mem-

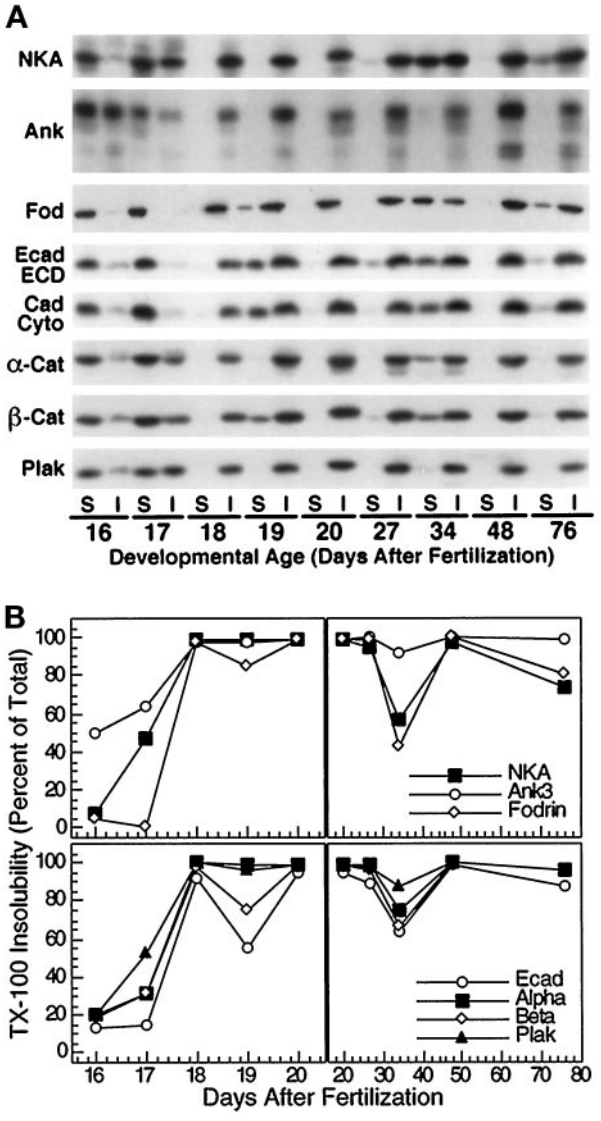

Figure 2. Development of Triton X-100 insolubility of proteins during kidney development. (A) Kidneys of different embryonic and postnatal ages were homogenized in buffers containing 0.5% Triton X-100. Homogenates were then centrifuged at 15,000 × *g* to generate soluble and insoluble fractions. For each developmental age, equal volumes of each fraction (S, Triton X-100 soluble; I, Triton X-100 insoluble) were separated on 5% (ank3 and fod) or 7.5% (NKA, Ecad ECD, Ecad Cyto, α-cat, β-cat, and plak) SDS-polyacrylamide gels and then electroblotted to nitrocellulose filters. Nitrocellulose filters were then probed with polyclonal antibodies specific for Na/K-ATPase (NKA), ankyrin-3 (ank3), nonerythroid spectrin (fodrin, fod), E-cadherin extracellular domain (Ecad ECD), E-cadherin cytoplasmic domain (Ecad Cyto), α-catenin (α-cat), β-catenin (β-cat), or plakoglobin (plak). Specific protein bands at appropriate molecular sizes were observed in all cases. Ankyrin-3 immunoblot shows both 190-kDa (bottom doublet) and 220-kDa (upper band) splice variants of Ankyrin-3. Note that β-catenin and plakoglobin protein bands in Triton X-100–insoluble fractions exhibit slower electrophoretic mobility relative to protein in Triton X-100 soluble fractions. (B) Autoradiograms shown in A were subjected to scanning densitometry. Data are expressed as percent Triton X-100 insoluble for each protein and time point and plotted against developmental age (days after fertilization). Left, time points before birth; right, time points after birth. Data for Na/K-ATPase, ankyrin-3, and fodrin are plotted in the top two panels. Because the 190- and 220-kDa splice variants of ankyrin-3 became Triton X-100 insoluble with identical kinetics, data for the two were combined. Data for E-cadherin, α-catenin, β-catenin, and plakoglobin are plotted in the bottom two panels. Antisera directed against extracellular and cytoplasmic domains of E-cadherin detected single bands of identical molecular sizes (~120 kDa), which displayed similar kinetics for development of Triton X-100 insolubility. Therefore, data for the two were averaged, and the resulting averaged data are shown in the bottom two panels (Ecad).

branes (Hoock *et al.*, 1997). Likewise, we focused our efforts on fodrin rather than erythroid spectrin, because previous investigations have revealed that it is the major spectrin paralogue in kidney (Piepenhagen *et al.*, 1995).

The protein level of Na/K-ATPase increased dramatically during kidney development, with most of the increase occurring between birth and 4 wk after birth. In contrast, the level of the 220-kDa splice variant of ankyrin-3 increased markedly during embryonic time points, declined at the time of birth, and then increased again to a maximum at 4 wk after birth. Unlike the 220-kDa splice variant of ankyrin-3, the protein level of the 190-kDa splice variant of ankyrin was essentially identical to that of Na/K-ATPase during development. The amount of fodrin increased significantly during embryogenesis, declined around the time of birth, and then increased steadily throughout postnatal development, reaching a maximum at 8 wk after birth; the reason for the decrease in fodrin level at E19 is not understood at present but does not appear to be an artifact of tissue or sample preparation.

The protein level of E-cadherin increased steadily throughout embryonic and early postnatal development, reaching a maximum at 2 wk after birth and then declined slightly by 8 wk after birth. Protein levels of α-catenin and β-catenin did not vary much during this developmental process (two- to threefold maximal increase) except at 76 d, when the level of β-catenin was low but detectable. The protein level of plakoglobin increased approximately sevenfold during kidney development.

Triton X-100 Insolubility of Proteins During Kidney Development

It has been demonstrated previously that the membrane cytoskeleton is resistant to extraction with buffers containing 0.5% Triton X-100. Therefore, we examined the kinetics with which proteins became resistant to Triton X-100 extraction during kidney development (Figure 2); data obtained from the analysis of CD1 mice are shown, but similar trends in the development of Triton X-100 insolubility were also observed in C57Bl/6 mice. In this study, mild sonication was re-

quired to ensure that Triton X-100 extracted cells throughout the tissue. Note that in previous studies, we did not sonicate MDCK cells to "solubilize" protein. The sonication conditions used in the present study may be harsher, but nevertheless we find that the proteins analyzed become resistant to extraction with Triton X-100 consistent with our previous studies with MDCK cells.

Na/K-ATPase was almost completely Triton X-100 soluble on E16. By E18, however, Na/K-ATPase was already nearly 100% Triton X-100 insoluble. Na/K-ATPase remained Triton X-100 insoluble until 2 wk after birth, at which time its Triton X-100 insolubility declined somewhat (~60% insoluble). The amount of Na/K-ATPase present in the Triton X-100–insoluble fraction subsequently returned to 100% at 4 wk after birth and then decreased slightly as adulthood was reached. E-cadherin and catenins developed Triton X-100 insolubility with kinetics similar to that of Na/K-ATPase. E-cadherin and catenins became Triton X-100 insoluble between E16 and E18 and remained largely insoluble thereafter except at 2 wk after birth when their Triton X-100 insolubility decreased. Despite these general similarities, these proteins differed in their overall level of resistance to Triton X-100 extraction, with E-cadherin being least insoluble at all time points, plakoglobin being most insoluble, and α- and β-catenin being intermediate. Note that Na/K-ATPase, E-cadherin, and catenins displayed similar kinetics for development of Triton X-100 insolubility, and Triton X-100–insoluble β-catenin and plakoglobin displayed retarded electrophoretic mobility.

Fodrin became 100% Triton X-100 insoluble by E18 and retained this level of insolubility at all subsequent time points except 2 wk after birth, similar to the time course of Triton X-100 insolubility of Na/K-ATPase, E-cadherin, and catenins. There was, however, one difference between fodrin and the other proteins. Although Triton X-100 insolubility increased linearly between E16 and E18 for other proteins, fodrin remained completely soluble up to E17 and then very rapidly became Triton X-100 insoluble between E17 and E18. In contrast to Na/K-ATPase, fodrin, E-cadherin, and catenins, a large percentage of ankyrin-3 (50%) was already Triton X-100 insoluble at E16. Between E16 and E18, this percentage increased from 50% to 100%. Ankyrin-3 remained resistant to extraction with Triton X-100 at all time points thereafter, never becoming <92% Triton X-100 insoluble even at 2 wk after birth when most of the other proteins had become less resistant to Triton X-100 extraction. Because ankyrin is highly sensitive to proteolysis, and immunoblots for all proteins were obtained by splitting single samples equally among multiple gels, it is very unlikely that the observed decrease in the amount of ankyrin insoluble in Triton X-100 at 2 wk after birth is due to protein degradation.

Protein Localization During Kidney Development

Immunohistochemical localization of Na/K-ATPase, ankyrin-3, fodrin, E-cadherin, and catenins was examined in frozen kidney sections from E16, neonatal, and 1-, 2-, 4-, and 8-wk-old CD1 mice. For brevity, only immunofluorescence staining for Na/K-ATPase, ankyrin-3, fodrin, and E-cadherin in sections of neonatal kidney is shown in Figure 3. Within sections from kidneys of this age, all stages of renal epithelial differentiation can be observed. In all cases, sections were subjected to double immunofluorescence staining with a monoclonal antibody directed against cytokeratin 8 (Figure 3, fluorescein staining in B, D, F, and H). Other studies have shown that cytokeratin 8 expression is an early marker of mesenchymal-to-epithelial conversion in developing kidney (Holthofer *et al.*, 1984), and we previously demonstrated that it is specifically expressed within distal segments of mature nephrons (Piepenhagen *et al.*, 1995).

Figure 3, A and B, shows staining for Na/K-ATPase either alone (Figure 3A) or as a double exposure with cytokeratin 8 staining (Figure 3B). Although every cell must express a certain low level of Na/K-ATPase to maintain ionic homeostasis, it is clear that the amount of Na/K-ATPase immunoreactivity varies greatly among epithelial cells at different stages of differentiation. Na/K-ATPase was not expressed above background levels in early nephrogenic structures (cellular aggregates and comma- and S-shaped bodies). This is illustrated by the comma-shaped body present in the upper right hand corner of Figure 3, A and B (asterisks), and by a number of other early nephrogenic structures present near the bottom left corner (arrows). As can be seen in Figure 3B, cells within comma-shaped bodies and other early structures began to express weak cytokeratin 8 staining along their basal and apical surfaces. This staining was diagnostic and aided in the identification of these structures (see above). Collecting ducts and the branching ureteric system from which they are derived also failed to stain above background levels for Na/K-ATPase. Developing collecting ducts were identified in Figure 3, A and B, by their intense apical cytokeratin 8 staining and by their relatively small diameter (~20 μm) and somewhat polygonal shape. In contrast, most other tubules in Figure 3, A and B, exhibited significant staining for Na/K-ATPase. This staining was restricted to basal-lateral plasma membranes in all cases, as confirmed by double immunofluorescence with antibody to the tight junction marker ZO-1. Some tubules stained much more intensely than others, but interpretation of these differences was difficult, because they could reflect formation of different nephron segments and/or differences in developmental state within the same segment. Tubular morphology and cytokeratin 8 staining patterns led us to conclude, however, that at

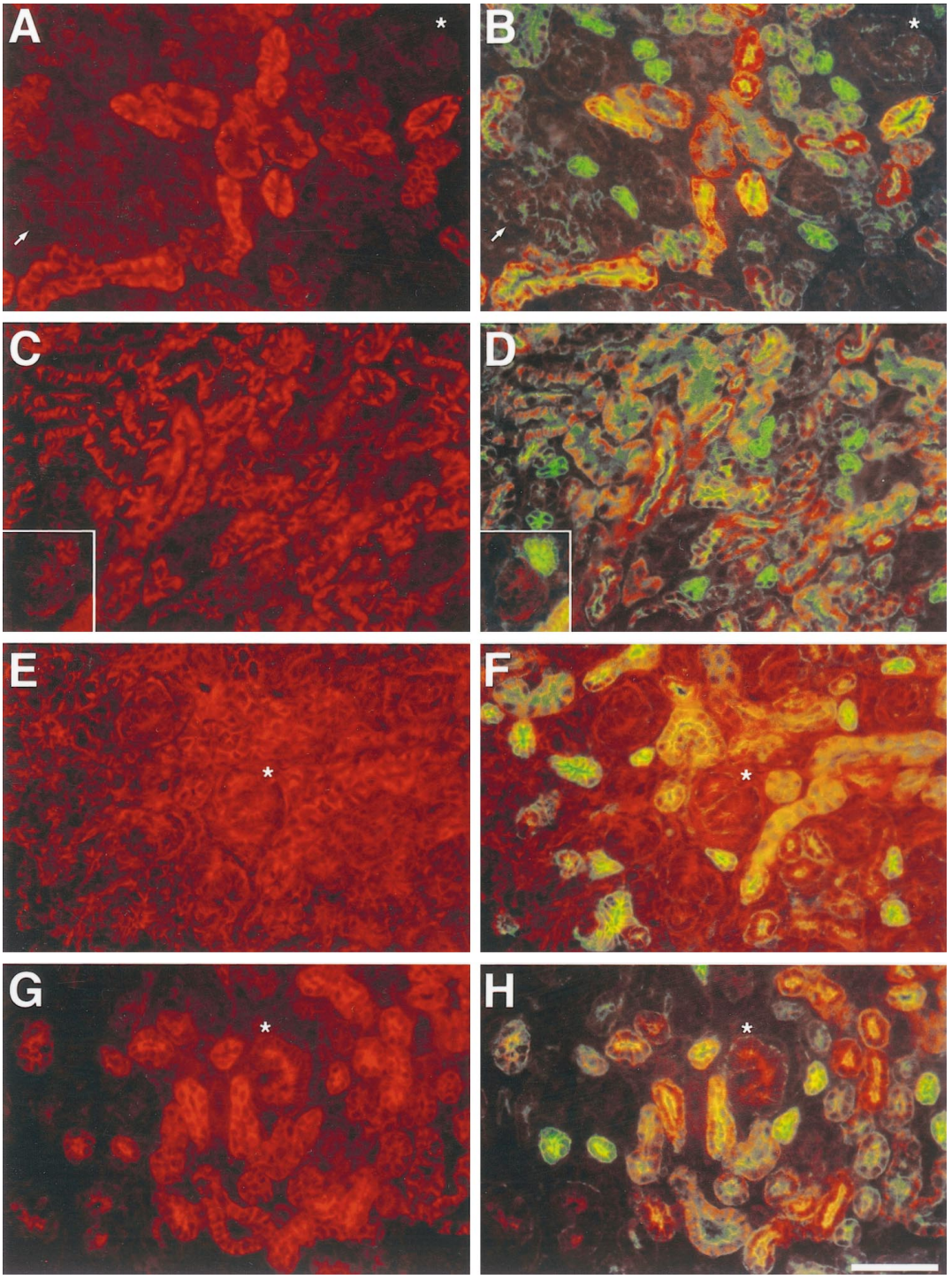

Figure 3. Protein localization during kidney development. Kidney sections from neonatal CD1 mice were subjected to double immunofluorescence with polyclonal antibodies to Na/K-ATPase, ankyrin-3, fodrin, E-cadherin, and a monoclonal antibody to cytokeratin 8. (A, B) Field from neonatal kidney that was subjected to double immunofluorescence with anti-Na/K-ATPase and anti-cytokeratin 8 antibodies. Na/K-ATPase was detected using a rhodamine-labeled secondary antibody, and cytokeratin 8 was detected using a fluorescein-labeled secondary antibody. (A) Na/K-ATPase staining alone; (B) double exposure for Na/K-ATPase and cytokeratin 8 staining. (C, D) Field from neonatal kidney that was subjected to double immunofluorescence with antibodies to ankyrin-3 and cytokeratin 8. Ankyrin-3 was detected using a rhodamine-labeled secondary antibody, and cytokeratin 8 was detected using a fluorescein-labeled secondary antibody. Ankyrin-3 staining is shown alone (C) or as a double exposure with cytokeratin 8 staining (D). Insets in C and D show a comma-shaped body from a

least some of them were developing distal convoluted tubules that express high amounts of Na/K-ATPase in the adult kidney (Katz *et al.*, 1979; Kashgarian *et al.*, 1985; Piepenhagen *et al.*, 1995).

Figure 3, C and D, shows immunofluorescence staining for ankyrin-3 alone (Figure 3C) or in combination with cytokeratin 8 (Figure 3D). Ankyrin-3 was weakly stained in early nephrogenic structures. Examples are shown in Figure 3, C and D, insets, in which a comma-shaped body can be seen next to a branch of the ureteric system. The ureteric tubule is the structure that exhibits strong cytokeratin 8 staining along all plasma membranes, with some enrichment along lumenal and apical membranes. Ankyrin-3 staining within ureteric tubules was slightly stronger than that in comma- and S-shaped bodies and was primarily localized along lateral plasma membranes. This lateral staining was slightly more intense toward lumenal and apical ends of lateral membranes. In developing collecting ducts (identified as above; Figure 3, compare C and D), ankyrin-3 staining was barely above background and was restricted primarily to lateral plasma membranes. Unlike staining in ureteric tubules, this staining was of uniform intensity along the entire length of lateral membranes. This weak ankyrin-3 staining is consistent with the fact that only intercalated cells stain for ankyrin-3 within mature collecting ducts (Piepenhagen *et al.*, 1995). Ankyrin-3 staining in other developing epithelial tubules was much more pronounced than that in early nephrogenic structures, ureteric tubules, or collecting ducts. In all cases, staining was restricted to basal and lateral plasma membranes (confirmed by double immunofluorescence with ZO-1 antibody). Some of these tubules stained more intensely than others, but the difference among tubular staining intensities was not as great as in the case of Na/K-ATPase. Two of the tubules that stained more intensely can be seen just to the left of center in Figure 3, C and D. Based on their size, morphology, and pattern of cytokeratin 8 staining (primarily lumenal), these are most likely differentiating distal convoluted tubules, segments that stain intensely for ankyrin-3 in mature nephrons (Piepenhagen *et al.*, 1995). Less intensely staining tubules could be either differentiating proximal tubules or distal segments in earlier stages of development. The number of such tubules and the size and morphology of some of them argue that at least a portion are differentiating proximal tubules. If true, at least some of the tubules in Figure 3, A and B, that express less Na/K-ATPase are likely to be differentiating proximal tubules.

In contrast to Na/K-ATPase and ankyrin-3, fodrin immunofluorescence was present within all cell types in developing kidneys. This is obvious in Figure 3, E and F, which shows fodrin staining alone (Figure 3E) or as a double exposure with cytokeratin 8 staining (Figure 3F). Fodrin was expressed in comma-shaped bodies (asterisks) and other early nephrogenic structures. Within these structures, fodrin staining was associated primarily with lateral plasma membranes and was more intense toward lumenal and apical domains. Fodrin staining in developing collecting ducts and ureteric tubules was also mainly present along lateral plasma membranes but was uniform along their length. Collecting ducts were identified as above, and a branching ureteric tubule can be seen in Figure 3, E and F, bottom, near the left side. In Figure 3F, this tubule is identified by its prominent cytokeratin 8 staining, which is present along all plasma membranes but slightly enriched along apical membranes. Staining in differentiating proximal and distal tubules was also uniformly distributed along lateral plasma membranes. As in the case of Na/K-ATPase and ankyrin-3, subcellular localization of fodrin was confirmed in double immunofluorescence experiments with antibody to ZO-1. In all of the above structures, fodrin staining was of approximately equal intensity. In addition to its staining of epithelia, slightly weaker fodrin staining was also observed in nonpolarized mesenchymal cells. This staining was often diffuse but was sometimes associated with plasma membranes.

E-cadherin immunofluorescence is shown in Figure 3, G and H, either alone (Figure 3G) or in combination with cytokeratin 8 (Figure 3H). Previous studies have demonstrated that E-cadherin expression is one of the earliest markers of epithelial differentiation, beginning at the cellular aggregate stage (Vestweber *et al.*, 1985). Our data are consistent with these findings. E-cadherin expression was already prominent in cellular aggregates, comma-shaped bodies (asterisks), and S-shaped bodies. Weak staining was observed within basal and lateral plasma membranes. In addition, intense staining was seen at or near forming lumens.

Figure 3 (facing page). different field immediately beneath a branch of the ureteric bud. The ureteric bud can be identified by its prominent cytokeratin 8 staining in D. (E, F) Field from neonatal kidney that was subjected to double immunofluorescence with anti-fodrin and anti-cytokeratin 8 antibodies. Fodrin was detected using a rhodamine-labeled secondary antibody, and cytokeratin 8 was detected using a fluorescein-labeled secondary antibody. (E) Fodrin staining alone; (F) double exposure for fodrin and cytokeratin 8 staining. (G, H) Field from neonatal kidney that was subjected to double immunofluorescence with antibodies to E-cadherin and cytokeratin 8. E-cadherin was detected using a rhodamine-labeled secondary antibody, and cytokeratin 8 was detected using a fluorescein-labeled secondary antibody. E-cadherin staining is shown alone (G) or as a double exposure with cytokeratin 8 staining (H). Asterisks mark comma-shaped bodies that are found immediately below them. Arrows in A and B point to other early nephrogenic structures that are identified by weak basal and apical cytokeratin 8 staining. All fields are shown at the same magnification. Bar, 50 μm.

Double immunofluorescence experiments with antibodies to E-cadherin and the tight junction marker ZO-1 demonstrated that E-cadherin staining did not extend above tight junctions. Identical subcellular staining patterns were observed in ureteric tubules and developing collecting ducts (identified as above; Figure 3, compare G and H). In differentiating proximal and distal tubules, E-cadherin staining was also observed and was restricted to basal and lateral plasma membranes. Instead of being concentrated at apical-lateral regions, however, this staining was distributed uniformly along lateral plasma membranes. These results indicate that during the process of renal epithelial cell differentiation, E-cadherin is initially concentrated at apical-lateral cell–cell junctions and subsequently becomes more evenly expressed along lateral membranes. One exception to this occurs at 4 wk after birth when a subset of proximal tubules stop expressing E-cadherin (see Figure 4H and description below). With this one exception, E-cadherin was expressed within all developing nephron segments, and its staining was of similar intensity in all cell types and tubules in which it was observed. We have also examined expression of plakoglobin and α- and β-catenin. α- and β-catenin displayed immunofluorescence staining patterns that mirrored those of E-cadherin, with the only difference being that α- and β-catenin staining was enriched near apical-lateral junctions in most differentiated nephron segments. Immunofluorescence colocalization of plakoglobin with desmoplakin and cytokeratin 8 indicated that, unlike β-catenin, plakoglobin was primarily associated with desmosomes in epithelial cells.

Relative Staining Intensities of Na/K-ATPase, Membrane Cytoskeleton, and E-cadherin Along Developing Nephrons

In a previous study, we presented data indicating that interaction with the membrane cytoskeleton might regulate not only the subcellular localization of Na/K-ATPase but also the amount of it present within basal-lateral membranes (Piepenhagen *et al.*, 1995). We wanted to know whether this might also occur in developing tubules. Therefore, we conducted double immunofluorescence histochemistry with an antibody to Na/K-ATPase and antibodies to ankyrin-3, fodrin, or E-cadherin. This allowed us to directly compare localization and relative staining intensities of Na/K-ATPase with those of the other proteins. Sections from E16, neonatal, and 1-, 2-, and 4-wk-old CD1 mouse kidneys were analyzed (Figure 4).

Figure 4, A–E, displays double immunofluorescence staining for Na/K-ATPase (fluorescein) and ankyrin-3 (rhodamine) in sections from E16, neonatal, and 1-, 2-, and 4-wk-old kidneys, respectively. In sections of E16 (Figure 4A) and neonatal (Figure 4B) kidney, ankyrin-3 was more widely distributed than Na/K-ATPase, consistent with data shown in Figure 3, A–D. At both developmental time points, tubules that possessed abundant ankyrin-3 staining and very little Na/K-ATPase staining could be observed. We believe these are developing convoluted and straight proximal tubules. In embryonic kidneys, it was somewhat difficult to distinguish these two segments because their characteristic tubular and cellular morphology was poorly developed. Nevertheless, we believe that morphological differences observed in Figure 4A reflect initial differentiation of these nephron segments. In neonatal kidneys (Figure 4B), these segments were more easily distinguished. Proximal convoluted tubules are large (40–50 μm diameter), irregularly elliptical in cross section, and possess extensive lateral plasma membrane interdigitations that run parallel to the basal-apical axis of tubules. In contrast, straight proximal tubules are of a slightly smaller diameter, display a more circular cross section, and lack lateral membrane interdigitations. Straight proximal tubules stained very weakly for Na/K-ATPase, but convoluted proximal tubules expressed significant amounts of Na/K-ATPase and appeared yellow throughout their basal-lateral plasma membranes (Figure 4B, large tubules in center).

Other tubules in Figure 4, A and B, expressed ankyrin-3 and large amounts of Na/K-ATPase. These appeared bright green throughout most of their basal-lateral domains and were of two types. Some were larger ($\sim$40 μm diameter) and irregularly shaped, and others were smaller ($\sim$25 μm) and of circular cross section. We believe the former are distal convoluted tubules, whereas the latter are ascending thick limbs of the loop of Henle. Identification is based on morphology and the fact that both of these nephron segments express large amounts of Na/K-ATPase in the adult (Katz *et al.*, 1979; Kashgarian *et al.*, 1985; Piepenhagen *et al.*, 1995). Yet other tubules in Figure 4, A and B, expressed ankyrin-3 and intermediate amounts of Na/K-ATPase and appeared orange or orange-yellow. In embryonic kidneys (Figure 4A), it was difficult to know whether these were developing proximal or distal convoluted tubules. In neonatal kidneys (Figure 4B), however, size and morphology identified these as transitional segments between convoluted and straight proximal tubules. In Figure 4B, a small number of tubules appeared to possess significant Na/K-ATPase staining in the absence of detectable ankyrin-3 staining. These are initial segments of proximal tubules. One attached to its cognate glomerulus can be seen in the middle of Figure 4B just below the large yellow proximal convoluted tubule. Note that the glomerulus has weak ankyrin-3 staining and no Na/K-ATPase staining above background. Basal-lateral plasma membrane localization of Na/K-ATPase and fodrin within these segments in the absence of

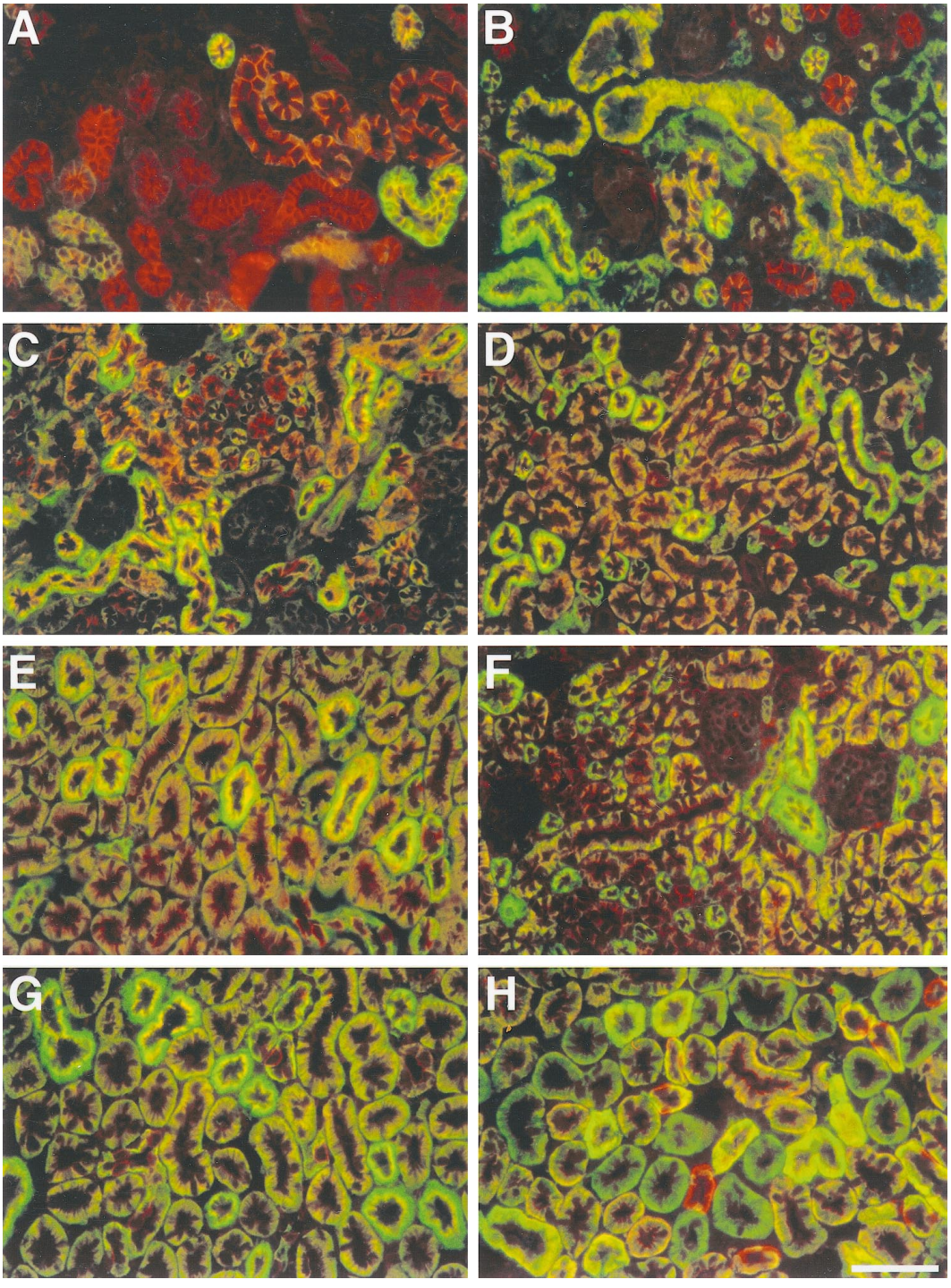

Figure 4. Relative staining intensities of Na/K-ATPase, membrane cytoskeleton, and E-cadherin along developing nephrons. Kidney sections from E16, neonatal, and 1-, 2-, and 4-wk-old CD1 mice were subjected to double immunofluorescence with polyclonal antibodies to ankyrin-3, fodrin, and E-cadherin and a monoclonal antibody to Na/K-ATPase. (A–E) fields from E16, neonatal, and 1-, 2-, and 4-wk-old kidneys, respectively, which were subjected to double immunofluorescence with antibodies to ankyrin-3 and Na/K-ATPase. Ankyrin-3 was detected using rhodamine-labeled secondary antibody, and Na/K-ATPase was detected using fluorescein-labeled secondary antibody. (F, G) Fields from 2- and 4-wk-old kidneys, respectively, that were subjected to double immunofluorescence with antibodies against fodrin and Na/K-ATPase. Fodrin was detected using rhodamine-labeled secondary antibody, and Na/K-ATPase was detected using fluorescein-labeled secondary antibody. (H) Field from 4-wk-old kidney that was subjected to double immunofluorescence with antibodies to E-cadherin and Na/K-ATPase. E-cadherin was detected with rhodamine-labeled secondary antibody, and Na/K-ATPase was detected using fluorescein-labeled secondary antibody. All fields are shown at the same magnification. Bar, 50 μm.

ankyrin-3 immunoreactivity suggests that a different ankyrin isoform is present.

At 1 wk after birth (Figure 4C), tubular segments were more differentiated morphologically, but general staining patterns for Na/K-ATPase and ankyrin-3 were similar to those observed in neonatal kidneys. One exception occurred in developing collecting ducts, which could be identified by their small size (~20 μm) and polygonal shape. For the first time, strong Na/K-ATPase staining appeared in this nephron segment. It was present within basal membranes and basal ends of lateral membranes within a subset of collecting duct cells. These must be principal cells, which, in the adult kidney, express Na/K-ATPase but not ankyrin-3 (Piepenhagen *et al.*, 1995). One other difference was that initial segments of proximal tubules now exhibited abundant ankyrin-3 staining, as evidenced by the fact that these segments now appeared orange rather than green in double exposures. By 2 wk after birth (Figure 4D), relative staining intensities of Na/K-ATPase and ankyrin-3 along differentiating nephrons were very similar. Again, the one exception occurred in collecting ducts. By this stage of development however, principal cells no longer stained for ankyrin-3, which was now strictly limited to intercalated cells as in the adult. At 4 wk after birth, staining patterns and relative staining intensities for Na/K-ATPase and ankyrin-3 had become even more similar and were now identical to those observed within mature nephrons.

Double immunofluorescence staining for Na/K-ATPase (fluorescein) and fodrin (rhodamine) in sections from 2- and 4-wk-old mice is shown in Figure 4, F and G. Fodrin staining patterns at these developmental time points were very similar to those for Na/K-ATPase in terms of subcellular localization and relative staining intensity. The only differences occurred in glomeruli and intercalated cells of collecting ducts, both of which displayed weak but significant fodrin staining while expressing only background levels of Na/K-ATPase. Staining intensities of fodrin and ankyrin-3 were also very similar (Figure 4, compare D and F with E and G). Three slight differences are weak fodrin staining in glomeruli, strong fodrin staining in principal cells of collecting ducts, and fodrin staining in initial segments of proximal tubules at early stages of development. Ankyrin-3 staining was not observed in any of these differentiating cell types or tubular segments. These differences are consistent with adult staining patterns and with wider distributions of fodrin found at early developmental stages in kidney (see Figure 3). Plasma membrane localization of fodrin in mesenchymal cells and early nephrogenic structures that lack ankyrin expression may be caused by association of fodrin with plasma membranes through ankyrin-independent membrane binding sites (Lombardo *et al.*, 1994).

In contrast to ankyrin-3 and fodrin, relative staining intensities of E-cadherin did not become more similar to those of Na/K-ATPase as development proceeded. If anything, they became less so. This is illustrated in Figure 4H, which shows a section from 4-wk-old kidney double stained for Na/K-ATPase (fluorescein) and E-cadherin (rhodamine). Abundant E-cadherin staining was observed in all cells of collecting ducts, distal convoluted tubules, and ascending thick limbs of the loop of Henle. E-cadherin expression was also observed in many proximal tubules. However, a large subpopulation of proximal tubules failed to stain with E-cadherin antibody, whereas staining for Na/K-ATPase was strong and the tubules therefore appeared green. These tubular segments must express ankyrin-3 and fodrin because such color patterns were never observed in double exposures with antibodies to Na/K-ATPase and these proteins. These segments were identified as initial segments of proximal tubules by morphology and fortuitous sections from 4-wk-old and adult kidneys that cut through glomeruli with their attached proximal tubules. This staining pattern is reminiscent of that of E-cadherin in adult C57Bl/6 mice in which initial segments of proximal tubule also failed to stain for E-cadherin (Piepenhagen *et al.*, 1995). However, the length of E-cadherin-deficient proximal tubule must be greater in CD1 than in C57Bl/6 mice based on the proportion of proximal tubular profiles that failed to stain for E-cadherin. At 2 wk after birth and at all earlier time points, these segments expressed E-cadherin at levels similar to those found in other segments. They must therefore turn off expression of E-cadherin as they complete their final differentiation. Cells within these segments appeared morphologically identical to E-cadherin–expressing proximal tubule cells and displayed identical expression patterns for Na/K-ATPase, ankyrin-3, and fodrin, suggesting that they express another cadherin that substitutes for E-cadherin.

DISCUSSION

Roles of the Membrane Cytoskeleton in Development of Epithelial Cell Polarity

Studies with cultured MDCK cells have demonstrated that the mechanism of selective retention operating either alone or in concert with TGN sorting can generate a restricted basal-lateral membrane distribution of Na/K-ATPase (Hammerton *et al.*, 1991; Mays *et al.*, 1995). In kidney, the model of selective retention predicts that ankyrin, fodrin, and E-cadherin should be expressed everywhere Na/K-ATPase is, and that all of these proteins should colocalize at the basal-lateral plasma membrane. The model further predicts that relative expression levels of Na/K-ATPase, ankyrin, and fodrin should vary in parallel among different

structures and segments and that assembly of a stable membrane cytoskeleton and association of other proteins with it should be reflected in acquisition of Triton X-100 insolubility. Data presented in this study are consistent with these predications.

The kinetics with which Na/K-ATPase, E-cadherin, and catenins become Triton X-100 resistant are dynamic and similar, indicating that they all associate with the same Triton X-100–insoluble cytoskeletal structure. Previous findings in vitro and with cultured cells suggest this structure is the membrane cytoskeleton (Nelson and Veshnock, 1987; Nelson and Hammerton, 1989; Davis and Bennett, 1990a,b; Devarajan *et al.*, 1994). That Na/K-ATPase and E-cadherin associate in complexes with the membrane cytoskeleton in situ is suggested by their coexpression and colocalization. With minor exceptions, fodrin, ankyrin-3, and E-cadherin are all expressed within the same cells as Na/K-ATPase. They are all localized at basal-lateral plasma membranes at all developmental stages and in all nephrogenic structures and differentiating tubules in which they are expressed (Figures 3 and 4). Apical plasma membrane staining is never observed, even at the earliest developmental stages.

Our previous finding that relative staining intensities of Na/K-ATPase, ankyrin-3, and fodrin varied in parallel along adult nephrons suggested that in addition to controlling subcellular localization of Na/K-ATPase, the membrane cytoskeleton might also regulate amounts of Na/K-ATPase present within basal-lateral plasma membranes (Piepenhagen *et al.*, 1995). Our present data are consistent with this idea. As shown in Figure 3, relative staining intensities of Na/K-ATPase, ankyrin-3, and fodrin are rather different at early embryonic time points and become more similar during kidney development until they are almost identical by 4 wk after birth. Differences at early developmental time points can be accounted for by variations in initial times of expression (described below) and by expression of different splice variants of ankyrin-3 that could not be distinguished by immunofluorescence. From both a developmental and physiological standpoint, these data are of great importance. Variations in Na/K-ATPase expression and activity along mature nephrons distinguish different epithelial subtypes (Katz *et al.*, 1979; Kashgarian *et al.*, 1985; Piepenhagen *et al.*, 1995) and are essential for countercurrent multiplication and urine concentration (Torretti *et al.*, 1972; Vander, 1995).

Regulation of Na/K-ATPase expression by ankyrin-3 is also suggested by the almost exact correspondence between expression patterns of Na/K-ATPase and the 190-kDa splice variant of ankyrin-3 (Figure 1). Both proteins also become highly Triton X-100 insoluble before the time at which they are maximally expressed (Figure 2). These two sets of data suggest that the 190-kDa splice variant of ankyrin-3 links Na/K-ATPase to a preexisting Triton X-100–resistant membrane cytoskeleton at some point during its biosynthesis and/or transport to the cell surface. Immunofluorescence colocalization of Na/K-ATPase, ankyrin-3, and fodrin at basal-lateral plasma membranes (Figures 3 and 4) indicates that this occurs at the plasma membrane. Previous in vitro data and studies with MDCK cells have demonstrated interaction between Na/K-ATPase and a full-length (~220 kDa) isoform of ankyrin (Nelson and Veshnock, 1987; Nelson and Hammerton, 1989; Davis and Bennett, 1990a,b; Devarajan *et al.*, 1994). However, similar in vitro studies have not been conducted with the 190-kDa splice variant of ankyrin-3.

The increase in levels of the 220-kDa splice variant of ankyrin-3 correlates with development of Triton X-100 insolubility of Na/K-ATPase, E-cadherin, and catenins (Figure 2). These data indicate that accumulation of the 220-kDa splice variant of ankyrin-3 is rate limiting in the assembly of the Triton X-100 insoluble membrane cytoskeleton. This assertion is further supported by the following two observations. First, ankyrin-3 is relatively Triton X-100 insoluble at the earliest times examined (E16), even though other proteins are almost completely soluble (Figure 2). Second, immunofluorescence reveals that fodrin is more widely distributed during early renal development than ankyrin-3 (Figure 4) and that significant Na/K-ATPase staining is only observed in differentiating epithelial cells after ankyrin-3 begins to accumulate (Figures 3 and 4). In contrast, fodrin expression is relatively constant during development of Triton X-100 insolubility of Na/K-ATPase, E-cadherin, and catenins, and its resistance to Triton X-100 extraction increases abruptly when expression of the 220-kDa splice variant of ankyrin-3 increases. This indicates that some threshold of ankyrin expression or membrane cytoskeleton reorganization may have to be reached before fodrin becomes stably integrated into a Triton X-100 insoluble membrane cytoskeleton. Although the 220-kDa splice variant of ankyrin-3 appears to be a rate-limiting factor during assembly of the membrane cytoskeleton, it cannot be the only one. Were this the case, it should be 100% Triton X-100 insoluble at the earliest times examined (E16, Figure 2). It is not, indicating that mechanisms involving expression of other essential components or posttranslational modifications of these proteins must also regulate assembly of the membrane cytoskeleton.

Roles of E-cadherin in the Development of Epithelial Cell Polarity

Previous studies using MDCK cells have indicated that E-cadherin–mediated cell–cell adhesion provides the initial positional cue to organize the membrane cytoskeleton and other cellular machinery (McNeill *et*

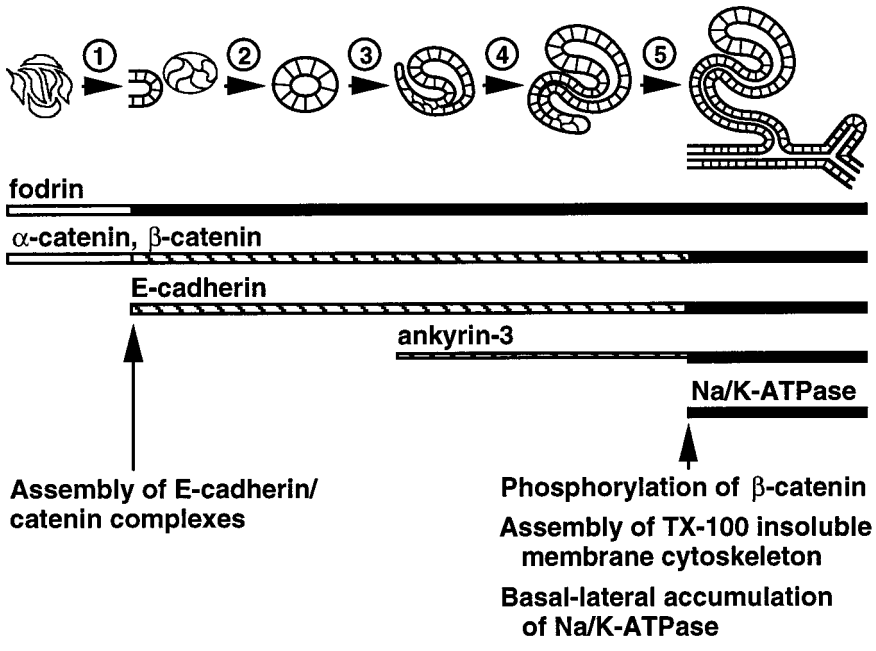

Figure 5. Model of membrane cytoskeleton assembly and basal-lateral accumulation of Na/K-ATPase in the renal epithelium in situ. The schematic time line at the top depicts different stages of early renal epithelial differentiation (nonpolarized mesenchymal cells, cellular aggregates, renal vesicles, comma-shaped bodies, S-shaped bodies, and early tubules, from left to right). The numbers above the arrows identify different events during renal epithelial differentiation: (1) induction and compaction of mesenchymal cells; (2) initial polarization and lumen formation; (3) elongation of renal vesicles and morphological transformation into comma-shaped bodies; (4) elongation and morphological transformation of comma-shaped bodies into S-shaped bodies; (5) fusion of S-shaped bodies with the ureteric system to form early tubules. Horizontal bars below the schematic time line represent the times at which various proteins are expressed; thicker lines correspond to relatively higher levels of protein expression. Open bars represent diffuse cytosolic expression, striped bars represent apical-lateral membrane expression, and filled bars represent uniform lateral membrane expression. Arrows and text at the bottom indicate times at which important events are thought to occur during development of E-cadherin–mediated cell–cell adhesion and assembly of the membrane cytoskeleton.

al., 1990, 1993; Nelson *et al.*, 1990). Our data are consistent with this idea. Immunofluorescence reveals that E-cadherin is restricted to basal-lateral plasma membranes and is expressed in differentiating epithelial cells before the accumulation of ankyrin-3 and Na/K-ATPase. Initially, E-cadherin staining is localized to apical-lateral membrane boundary and later becomes more uniformly distributed along lateral plasma membranes. It may be that during initial stages of differentiation, E-cadherin plays a role in organizing apical-lateral membrane junctions. Such junctional complexes may include tight junctions, structures that are localized at apical-lateral membrane boundaries at these times and require cadherin activity to form (Gumbiner and Simons, 1986; Gumbiner *et al.*, 1988; Schnabel *et al.*, 1990). Uniform E-cadherin expression along lateral plasma membranes could subsequently provide the positional information to organize the membrane cytoskeleton. This idea is supported by the fact that significant accumulation of ankyrin-3 and Na/K-ATPase is first observed in early tubules (those that have not yet differentiated into distinct proximal and distal segments), the stage at which E-cadherin staining becomes uniformly distributed along lateral membranes. Although E-cadherin expression patterns are consistent with a role for E-cadherin in controlling localization of the membrane cytoskeleton, they are not consistent with it controlling amounts of membrane cytoskeleton present at basal-lateral plasma membranes. Relative E-cadherin staining intensities do not vary much along developing nephrons and do not come to resemble those of Na/K-ATPase, ankyrin-3, and fodrin (Figure 4).

It has been demonstrated in other systems that association of α- and β-catenin with E-cadherin is required for E-cadherin activity (Nagafuchi and Takeichi, 1988; McNeill *et al.*, 1990; Ozawa *et al.*, 1990). Our findings that E-cadherin is primarily localized to plasma membranes and colocalized with α- and β-catenin in all cell types and at all developmental stages suggest that E-cadherin observed in our studies is associated with α- and β-catenin. Expression profiles of E-cadherin and α- and β-catenin (Figure 1) reveal that expression of E-cadherin increases considerably during kidney development, whereas expression of α- and β-catenin remain relatively constant. It follows that at early time points when E-cadherin expression is low there should exist pools of α- and β-catenin uncomplexed with E-cadherin. Alternatively, another cadherin may be expressed that does not react with either cadherin antibody used in our study. For example, cadherin-11 is expressed in uninduced mesenchyme at this time, and cadherin-6 is expressed in early differentiating epithelial cells that give rise to proximal tubules (Cho *et al.*, 1998). Regulation of cadherin–catenin complexes by posttranslational modification of catenins is suggested by the observation that both β-catenin and plakoglobin present within Triton X-100–insoluble fractions display retarded electrophoretic mobilities relative to

protein present in the Triton X-100–soluble fractions (Figure 2). This retarded electrophoretic mobility can be partially reversed by treating fractions with a tyrosine phosphatase, indicating that it is caused by phosphorylation and suggesting that Triton X-100–insoluble β-catenin and plakoglobin may also be phosphorylated on serine and threonine. These data suggest that phosphorylation of armadillo family members may regulate association of cadherin–catenin complexes with the Triton X-100–insoluble cytoskeleton.

Conclusions

Based on the data presented in this study, we propose the following model for assembly and localization of the membrane cytoskeleton and Na/K-ATPase in situ (Figure 5). Before induction by the ureteric bud, mesenchymal cells express abundant fodrin and α- and β-catenin. Upon induction, E-cadherin expression begins. Newly synthesized E-cadherin immediately binds to uncomplexed α- and β-catenin and is transported to the cell surface where it forms homotypic contacts with E-cadherin molecules on adjacent cells, thereby defining the future lateral plasma membrane. At slightly later times (S-shaped body stage) expression of the 220-kDa splice variant of ankyrin-3 begins. Phosphorylation of β-catenin in E-cadherin–catenin complexes may render these complexes capable of interacting with 220-kDa ankyrin-3. This interaction induces assembly of a stable Triton X-100–insoluble membrane cytoskeleton specifically beneath basal-lateral plasma membranes. At yet later times (early tubules), expression of the 190-kDa splice variant of ankyrin-3 begins to increase. Interaction of this splice variant of ankyrin-3 with Na/K-ATPase allows Na/K-ATPase to be integrated into the Triton X-100–resistant membrane cytoskeleton, thereby leading to its stabilization and accumulation. These results indicate that assembly and basal-lateral accumulation of E-cadherin–mediated adherens junctions, the membrane cytoskeleton, and Na/K-ATPase is regulated in kidney epithelial cells in situ through sequential protein expression. In contrast, cultured renal epithelial cells constitutively express these protein components, which become reorganized to the basal-lateral membrane upon E-cadherin–mediated cell–cell adhesion. Despite this difference in the timing of expression of different proteins, renal epithelial cells in culture and in situ achieve the same end point distribution of membrane and membrane-cytoskeletal proteins.

Results presented in this study are consistent with the hypothesis that the mechanism of selective retention operates in situ during renal epithelial development and helps control intra- and intercellular expression of Na/K-ATPase. It is interesting to note that during renal ischemia in rodents (Doctor *et al.*, 1993) and humans (Alejandro *et al.*, 1995), cell surface Na/K-ATPase in proximal tubules is rapidly lost and protein appears inside the cells. This correlates with loss of membrane cytoskeleton components from beneath basal-lateral plasma membranes (Alejandro *et al.*, 1995) and their degradation (Doctor *et al.*, 1993). These observations are consistent with the data presented here that interaction with the membrane cytoskeleton plays a crucial role in controlling the subcellular localization and plasma membrane stability of Na/K-ATPase.

ACKNOWLEDGMENTS

We thank the following for their generous gifts of antibodies. Kathleen Siemers prepared the polyclonal antisera to the α-subunit of Na/K-ATPase and the cytoplasmic domain of E-cadherin. Dr. Inke Näthke provided the antibodies to α- and β-catenin. Drs. Lindsey Hinck and Jackie Papkoff provided the antiserum to plakoglobin. Drs. Luanne Peters and Samuel Lux provided the ankyrin-3 antiserum. Dr. Rolf Kemler provided the antibody to the extracellular domain of E-cadherin. Drs. Kent Grindstaff and Robert Mercer provided the monoclonal antibody to the α-subunit of Na/K-ATPase. In addition, we thank all of the members of this laboratory for their helpful discussions during the preparation of the manuscript. This work was supported by a grant from the National Institutes of Health to W.J.N. P.A.P. was supported by a grant from the Liebermann foundation.

REFERENCES

Alejandro, V.S., Nelson, W.J., Huie, P., Sibley, R.K., Dafoe, D., Kuo, P., Scandling, J.D.J., and Myers, B.D. (1995). Postischemic injury, delayed function and Na+/K+-ATPase distribution in the transplanted kidney. Kidney Int. *48*, 1308–1315.

Anderson, J.M., Stevenson, B.R., Jesaitis, L.A., Goodenough, D.A., and Mooseker, M.S. (1988). Characterization of ZO-1, a protein component of the tight junction from mouse liver and Madin-Darby canine kidney cells. J. Cell Biol. *106*, 1141–1149.

Brenner, B.M., and Rector, F.C. (1976). The kidney. In: The Kidney, vol. 1, ed. B.M. Brenner and F.C. Rector, Philadelphia: W.B. Saunders.

Brulet, P., Babinet, C., Kemler, R., and Jacob, F. (1980). Monoclonal antibodies against trophectoderm-specific markers during mouse blastocyst formation. Proc. Natl. Acad. Sci. USA *77*, 4113–4117.

Caplan, M.J., Anderson, H.C., Palade, G.E., and Jamieson, J.D. (1986). Intracellular sorting and polarized cell surface delivery of Na^+/K^+-ATPase, an endogenous component of MDCK cell basolateral plasma membranes. Cell *46*, 623–631.

Cho, E.A., Patterson, L.T., Brookhiser, W.T., Mah, S., Kintner, C., and Dressler, G.R. (1998). Differential expression and function of cadherin-6 during renal epithelium development. Development *125*, 803–812.

Davis, J., and Bennett, V. (1990a). The anion exchanger and Na+, K+, ATPase interact with distinct sites on ankyrin in in vitro assays. J. Biol. Chem. *265*, 17252–17256.

Davis, L.H., and Bennett, V. (1990b). Mapping the binding sites of human erythrocyte ankyrin for the anion exchanger and spectrin. J. Biol. Chem. *265*, 10589–10596.

Devarajan, P., Scaramuzzino, D.A., and Morrow, J.S. (1994). Ankyrin binds to two distinct cytoplasmic domains of Na, K-ATPase α subunit. Proc. Natl. Acad. Sci. USA *91*, 2965–2969.

Doctor, R.B., Bennett, V., and Mandel, L.J. (1993). Degradation of spectrin and ankyrin in the ischemic rat kidney. Am. J. Physiol. *264*, C1003–C1013.

Ekblom, P. (1989). Developmentally regulated conversion of mesenchyme to epithelium. FASEB J. *3*, 2141–2150.

Gumbiner, B., and Simons, K. (1986). A functional assay for proteins involved in establishing an epithelial occluding barrier: identification of a uvomorulin-like polypeptide. J. Cell Biol. *102*, 457–468.

Gumbiner, B., Stevenson, B., and Grimaldi, A. (1988). The role of the cell adhesion molecule uvomorulin in the formation and maintenance of the epithelial junctional complex. J. Cell Biol. *107*, 1575–1587.

Hammerton, R.W., Krzeminski, K.A., Mays, R.W., Ryan, T.A., Wollner, D.A., and Nelson, W.J. (1991). Mechanism for regulating cell surface distribution of Na^+, K^+-ATPase in polarized epithelial cells. Science. *254*, 847–850.

Herrenknecht, K., Ozawa, M., Eckerskorn, C., Lottspeich, F., Lenter, M., and Kemler, R. (1991). The uvomorulin-anchorage protein α-catenin is a vinculin homologue. Proc. Natl. Acad. Sci. USA *88*, 9156–9160.

Hinck, L., Nelson, W.J., and Papkoff, J. (1994). Wnt-1 modulates cell-cell adhesion in mammalian cells by stabilizing beta-catenin binding to the cell adhesion protein cadherin. J. Cell Biol. *124*, 729–741.

Holthofer, H., Miettinen, A., Lehto, V.-P., Lehtonen, E., and Virtanen, I. (1984). Expression of vimentin and cytokeratin types of intermediate filament proteins in developing and adult human kidneys. Lab. Invest. *65*, 74–86.

Hoock, T.C., Peters, L.L., and Lux, S.E. (1997). Isoforms of ankyrin-3 that lack the NH_2-terminal repeats associate with mouse macrophage lysosomes. J. Cell Biol. *136*, 1059–1070.

Kashgarian, M., Biemesderfer, D., Caplan, M., and Forbrush, B. (1985). Monoclonal antibody to Na, K-ATPase: immunocytochemical localization along nephron segments. Kidney Int. *28*, 899–913.

Katz, A.I., Doucet, A., and Morel, F. (1979). Na/K-ATPase activity along the rabbit, rat, and mouse nephron. Am. J. Physiol. *237*, F114–F120.

Kemler, R., Brulet, P., Schnebelen, M.-T., Gaillard, J., and Jacob, F. (1981). Reactivity of monoclonal antibodies against intermediate filament proteins during embryonic development. J. Embryol. Exp. Morphol. *64*, 45–60.

Knudsen, K.A., and Wheelock, M.J. (1992). Plakoglobin, or an 83-kD homologue distinct from β-catenin, interacts with E-cadherin and N-cadherin. J. Cell Biol. *118*, 671–679.

Lombardo, C.R., Weed, S.A., Kennedy, S.P., Forget, B.G., and Morrow, J.S. (1994). Beta II-spectrin (fodrin) and beta I epsilon 2-spectrin (muscle) contain NH_2- and COOH-terminal membrane association domains (MAD1 and MAD2). J. Biol. Chem. *269*, 29212–29219.

Marrs, J.A., Napolitano, E.W., Murphy-Erdosh, C., Mays, R.W., Reichardt, L.F., and Nelson, W.J. (1993). Distinguishing roles of the membrane-cytoskeleton and cadherin mediated cell-cell adhesion in generating different Na^+, K^+-ATPase distributions in polarized epithelia. J. Cell Biol. *123*, 149–164.

Mays, R.W., Siemers, K.A., Fritz, B.A., Lowe, A.W., van Meer, G., and Nelson, W.J. (1995). Hierarchy of mechanisms involved in generating Na/K-ATPase polarity in MDCK epithelial cells. J. Cell Biol. *130*, 1105–1115.

McClean, I.W., and Nakane, P.K. (1974). Periodate-lysine-paraformaldehyde fixative: a new fixative for immunoelectron microscopy. J. Histochem. Cytochem. *22*, 1077–1083.

McNeill, H., Ozawa, M., Kemler, R., and Nelson, W.J. (1990). Novel function of the cell adhesion molecule uvomorulin as an inducer of cell surface polarity. Cell. *62*, 309–316.

McNeill, H., Ryan, T.A., Smith, S.J., and Nelson, W.J. (1993). Spatial and temporal dissection of immediate and early events following cadherin-mediated epithelial cell adhesion. J. Cell Biol. *120*, 1217–1226.

Morrow, J.S., Cianci, C.D., Ardito, T., Mann, A.S., and Kashgarian, M. (1989). Ankyrin links fodrin to the alpha subunit of Na, K-ATPase in Madin-Darby canine kidney cells and in intact renal tubule cells. J. Cell Biol. *108*, 455–465.

Nagafuchi, A., and Takeichi, M. (1988). Cell binding function of E-cadherin is regulated by the cytoplasmic domain. EMBO J. *7*, 3679–3684.

Nagafuchi, A., Takeichi, M., and Tsukita, S. (1991). The 102 kd cadherin-associated protein: similarity to vinculin and posttranscriptional regulation of expression. Cell *65*, 849–857.

Nathke, I.S., Hinck, L., Swedlow, J.R., Papkoff, J., and Nelson, W.J. (1994). Defining interactions and distributions of cadherin and catenin complexes in polarized epithelial cells. J. Cell Biol. *125*, 1341–1352.

Nelson, W.J., and Hammerton, R.W. (1989). A membrane-cytoskeletal complex containing Na+, K+-ATPase, ankyrin, and fodrin in Madin-Darby canine kidney (MDCK) cells: implications for the biogenesis of epithelial cell polarity. J. Cell Biol. *108*, 893–902.

Nelson, W.J., Shore, E.M., Wang, A.Z., and Hammerton, R.W. (1990). Identification of a membrane-cytoskeletal complex containing the cell adhesion molecule uvomorulin (E-cadherin), ankyrin, and fodrin in Madin-Darby canine kidney epithelial cells. J. Cell Biol. *110*, 349–357.

Nelson, W.J., and Veshnock, P.J. (1987). Ankyrin binding to $(Na^+ + K^+)$ATPase and implications for the organization of membrane domains in polarized cells. Nature. *328*, 533–536.

Nelson, W.J., and Veshnock, P.J. (1986). Dynamics of membrane-skeleton (fodrin) organization during development of polarity in Madin-Darby canine kidney epithelial cells. J. Cell Biol. *103*, 1751–1765.

Ozawa, M., Ringwald, M., and Kemler, R. (1990). Uvomorulin-catenin complex formation is regulated by a specific domain in the cytoplasmic region of the cell adhesion molecule. Proc. Natl. Acad. Sci. USA *87*, 4246–4250.

Pasdar, M., and Nelson, W.J. (1988). Kinetics of desmosome assembly in Madin-Darby canine kidney epithelial cells: temporal and spatial regulation of desmoplakin organization and stabilization upon cell-cell contact. II. Morphological analysis. J. Cell Biol. *106*, 687–695.

Peifer, M., McCrea, P.D., Green, K.J., Wieschaus, E., and Gumbiner, B.M. (1992). The vertebrate adhesive junction proteins β-catenin and plakoglobin and the *Drosophila* segment polarity gene *armadillo* form a multigene family with similar properties. J. Cell Biol. *118*, 681–691.

Peters, L.L., John, K.M., Lu, F.M., Eicher, E.M., Higgins, A., Yialamas, M., Turtzo, L.C., Otsuka, A.J., and Lux, S.E. (1995). Ank3 (epithelial ankyrin), a widely distributed new member of the ankyrin gene family and the major ankyrin in kidney, is expressed in alternatively spliced forms, including forms that lack the repeat domain. J. Cell Biol. *130*, 313–330.

Piepenhagen, P.A., and Nelson, W.J. (1993). Defining E-cadherin-associated protein complexes in epithelial cells: plakoglobin, β- and γ-catenin are distinct components. J. Cell Sci. *104*, 751–762.

Piepenhagen, P.A., Peters, L.L., Lux, S.E., and Nelson, W.J. (1995). Differential expression of Na^+-K^+-ATPase, ankyrin, fodrin, and

E-cadherin along the kidney nephron. Am. J. Physiol. *269*, C1417–C1432.

Rodriguez-Boulan, E., and Nelson, W.J. (1989). Morphogenesis of the polarized epithelial cell phenotype. Science *245*, 718–725.

Saxen, L., and Sariola, H. (1987). Early organogenesis of the kidney. Pediatr. Nephrol. *1*, 385–392.

Schnabel, E., Anderson, J.M., and Farquhar, M.G. (1990). The tight junction protein ZO-1 is concentrated along slit diaphragms of the glomerular epithelium. J. Cell Biol. *111*, 1255–1263.

Stevenson, B.R., Siliciano, J.D., Mooseker, M.S., and Goodenough, D.A. (1986). Identification of ZO-1: a high molecular weight polypeptide associated with the tight junction (Zonula occludens) in a variety of epithelia. J. Cell Biol. *103*, 755–766.

Torretti, J., Hendler, E., Weinstein, E., Longnecker, R.E., and Epstein, F.H. (1972). Functional significance of Na-K-ATPase in the kidney: effects of ouabain inhibition. Am. J. Physiol. *222*, C1398–C1405.

Vander, A.J. (1995). Renal Physiology, vol. 1, New York: McGraw-Hill, 238.

Vestweber, D., and Kemler, R. (1984). Rabbit antiserum against a purified surface glycoprotein decompacts mouse preimplantation embryos and reacts with specific adult tissues. Exp. Cell Res. *152*, 169–178.

Vestweber, D., Kemler, R., and Ekblom, P. (1985). Cell-adhesion molecule uvomorulin during kidney development. Dev. Biol. *112*, 213–221.